A Biosensor for Hydrogen Peroxide Based on Single walled Carbon Nanotube and Metal Oxide Modified Indium Tin Oxide Electrode

A.K. Upadhyay, Shen-Ming Chen[*], Tzu-Wei Ting, Ya-Yu Peng

Department of Chemical Engineering and Biotechnology, National Taipei University of Technology, No.1, Section 3, Chung-Hsiao East Road , Taipei 106, Taiwan (ROC).
[*]E-mail: smchen78@ms15.hinet.net

A novel approach has been developed for a highly sensitive, fast responding and stable monoenzymatic amperometric biosensor for the detection of hydrogen peroxide using coimmobilized the single walled carbon nanotube (SWNT) and methylene blue (MB) into the metal oxide (SnO_2) derived organically modified sol-gel glasses (ormosil). Nafion (NAF) was dispersed within the ormosil matrix to enhance the electron transportation in the modified film. Horseradish peroxidase (HRP) was diffusionally adsorbed onto the SWNT/ormosil modified ITO (Indium tin oxide) electrode surface. The SWNT/ormosil-modified electrodes were characterized with scanning electron microscopy (SEM), Atomic Force microscopy (AFM) and UV-vis spectroscopy. Cyclic voltammetry and amperometry measurements were used to study and optimize the performance of the resulting peroxide biosensor. The apparent Michaelis-Menten constant was determined to be 1.6mM. The effect of pH, SWNT content, applied potential and temperature on the peroxide biosensor has been systemically studied. The fabricated biosensor had a fast response of H_2O_2, less than 5s and excellent linear range of concentration from 5×10^{-7} to 1×10^{-4}M with the detection limit of 0.3μM (S/N=3) under the optimum conditions. These results show that this amperometric biosensor could be used for the measurement of H_2O_2 in cellular, enzyme systems or cancer cell studies without the help of any fluorescent probes or detection reagents.

1. INTRODUCTION

The highly sensitive, selective and accurate analytical detection of hydrogen peroxide is of great relevance, because it is not only a by-product of several highly selective oxidases, but also an essential mediator in food, pharmaceutical, clinical, industrial, environmental analysis and many other

fields [1, 2]. Several analytical techniques such as titrimetry [3], spectrometry [4], chemiluminescence [5] and electrochemical methods [6, 7] have been developed to monitor H_2O_2. The first four methods suffer from a variety of drawbacks including interferences, long pre-treatments of the sample and in many cases these methods require the utilization of toxic or expensive reagents. Electrochemical methods, such as amprometric biosensors based on simple and economical immobilized redox proteins or enzymes modified electrodes have been extensively employed for determination of H_2O_2 for their simplicity, highly selective and intrinsic sensitivity [8, 9]. Nowadays, horseradish peroxidase (HRP) is being widely used in the fabrication of ormosil based amperometric biosensor for the detection of H_2O_2 due to its high purity, sensitivity, low cost and easy availability and high affinity to encapsulate into the ormosil film [10, 11].

Carbon nanotubes (CNTs) have attracted considerable studies since their discovery [12]. Due to their nanometric size, higher electrical conductivity, strong adsorptive ability, good mechanical strength, excellent biocompatibility, minimization of surface fouling, lack of toxicity and good electrocatalytic properties, currently, CNTs have received enormous attention in the biosensor field [13-15]. SWNTs modified biosensor offer substantially greater signals especially at low potential, reflecting the excellent electrocatalytic activity of SWNTs. Such low-potential operation of SWNTs based biosensor results in a wide linear range and fast response time. Several number of amperometric peroxide biosensors have been fabricated based on NAD^+ and SWNT modified electrode [16], CHIT/CAT/SWNT modified electrode [17], CoP-SWNT/GCE modified electrode [18], Polypyrrole/SWCNT-HRP nanocomposites modified electrode [19], SWNT/Prussian Blue/HRP modified electrode [20], DNA/Fc-SWNT/Au modified electrode [21],SWNT/ferritin/GCE modified electrode [22] and SWNT/CHIT/NAF/GCE modified electrode [23].

A series of water soluble organic dyes have been used as mediators in solution due to their excellent mediating ability and low cost. But in solution, dye molecule will pollute the reference electrode and counter electrode, and will also decrease the analytical sensing ability of sensor. Therefore, it would be preferable to immobilize the dye on the electrode surface. Several redox dyes such as, methylene green [24], meldola blue [25] and Celestine blue [26] can be used as electron transfer mediators, when immobilized on the electrode surfaces. The cracking of modified film and leaching out of biomolecules from the electrode surface are major drawbacks in the fabrication of electrochemical biosensor. To overcome these critical issues, we dispersed nafion within the metal oxide derived organically modified sol-gel glasses (ormosil) as a biocompatible matrix to encapsulate the dyes/biomolecules/SWNTs. The presence of nafion polymer in the ormosil matrix not only prevents the cracking and brittleness of the ormosil film but also improves the sensitivity and long term stability of biosensor [27]. Ormosils are the unique matrices to encapsulate the biomolecules [28, 29] due to their inert chemical nature, high mechanical strength, excellent optical properties, tunable porosity, strong adhesion properties to its surface support and easy modification.

In this article, we prepared a highly sensitive and selective H_2O_2 biosensor using three types of ormosil; 2-(3, 4-epoxycyclohexyl) ethyltrimethoxysilane (ETMOS) phenyltrimethoxysilane (PHTMOS), and 3-aminopropyltrimethoxysilane (APTMOS). Methylene blue (as redox mediator), SWNT and nafion were coimmobilized within the ormosil film. SnO_2 was incorporated within the matrix to enhance the surface area available for protein binding [30]. HRP was adsorbed onto the

SWNT modified electrode surface diffusionally. The widely present amino groups in APTMOS ormosil provide a hydrophilic microenvironment that is compatible with the biomolecules and increases the stability of the biosensor. The phenyl and epoxy group present as organic functionalities in ormosil provide better physical and mechanical strength to the ormosil matrix. Cyclic voltammetric and amperometric measurements were carried out to demonstrate the feasibility of MB as an electron shuttle between the immobilized peroxidase and electrode. SWNT was incorporated within ormosil facilitating the electron-transfer reaction between the enzyme and the electrode.

2. EXPERIMENTAL SECTION

2.1. Reagents, materials and Apparatus

Peroxidase from horseradish (POD, EC 1.11.1.7 type VI) and tin oxide were obtained from Sigma; Methylene Blue (MB) and nafion (perfluorosulfonated ion-exchange resin, 5% (w/v) solution in a solution of 90% aliphatic alcohol and 10% water mixture) were purchased from Fluka. Phenyltrimethoxysilane , 3 – Aminopropyltrimethoxysilane , 2 - (3 , 4 – epoxycyclohexyl) ethyltrimethoxysilane, N,N-Dimethylformamide (DMF) and singlewalled carbon nanotubes (1-2nm diameter) were purchased from Aldrich Chemical Co. Hydrogen peroxide (30% w/v solution) was purchased from Wako Pure Industrial Co., Japan. The concentrations of more diluted hydrogen peroxide solutions were determined by titration with cerium (IV) to a ferroin end point. Phosphate buffer solutions (PBS) of various pH were prepared with 0.1 M KH_2PO_4 and 0.1 M Na_2HPO_4 with supporting electrolyte 0.1 M KCl. All other chemicals employed were of analytical grade. Double distilled water was used throughout this work.

The electrochemical measurements were performed with a computer controlled CHI750A (TX, USA) electrochemical system. Cyclic voltammetry and amperometric measurements were done with a three electrode system comprising the SnO_2/NAF/HRP, MB/SnO_2/NAF/HRP and SWNT/MB/SnO_2/NAF/HRP as a working electrode, an Ag/AgCl reference electrode and platinum wire as counter electrode in 5ml (0.1 M, pH 7.0) phosphate buffer solution. Hitachi scientific instruments (Japan) Model S-3000H scanning electron microscope, CPSM model (USA) atomic force microscope and Hitachi scientific instruments (Japan) Model U-3300 UV-vis spectrophotometer were used for surface image and UV-vis spectra measurements respectively.

2.3 Fabrication of SWNT/MB/SnO$_2$/NAF/HRP based biosensor for H$_2$O$_2$

Indium tin oxide (ITO) was washed with acetone and was dried for 10 minute at room temperature before the modification of the electrodes. Three types of ormosil-modified electrodes (OMEs) were fabricated based on the composition given in Table1.

(A) *SWNT/MB/SnO$_2$/NAF/HRP*- 70 µl of 3-aminopropyltrimethoxysilane, 20µl (1mM) of methylene blue (MB) and 200µl of doubly distilled water were mixed in a cell with constant stirring, followed by the addition of 30µl (1mg/ml) of SWNT and 5µl of nafion in the same solution and stirred

for 5 minute to get homogeneous solution. After that 30µl of SnO_2 (dissolved in acetic acid), 10µl of 2-(3, 4-epoxyctclohexyl) ethyltrimethoxysilane, 5µl of phenyltrimethoxysilane and 0.1N, 10µl HCl were mixed and stirred for 10 minutes to completion of hydrolysis. 8µl of the prepared homogeneous solution was added over the indium tin oxide (ITO) electrode followed by the SWNT modified ormosil formation for 4-5h at room temperature. After complete drying of modified electrode, it was immersed in the solution of (1mg/ml) HRP enzyme for 4h for the diffusion of enzyme molecules into SWNT modified ormosil matrix, and again was dried for 5h at room temperature.

    (B) MB/SnO₂/NAF/HRP- In this modified electrode, SWNT was not coimmobilized within the ormosil matrix. The rest of the process was same as that for modified electrode A.

    (C) SnO₂/NAF/HRP- In this modified electrode, SWNT and MB were not coimmobilized within the ormosil matrix. The rest of the process was same as that for modified electrode A.

Table 1. Composition of SWNT based Ormosil modified electrodes.

OMEs (µl)	NAF[f] (µl)	APTMOS[a] (µl)	ETMOS[b] (µl)	PHTMOS[c] (µl)	MB[d] (µl)	SnO₂ (µl)	DDWATER (µl)	SWNT[e] (µl)	HCL (µl)
1	5	70	10	5	20	30	200	30	10
2	5	70	10	5	20	30	200	-	10
3	5	70	10	5	-	30	200	-	10

[a]3-aminopropyltrimethoxysilane;[b]2-(3,4-epoxycyclohexyl)ethyltrimethoxysilane;
[c] phenyltrimethoxysilane;[d] methylene Blue; [e]SWNT- Single walled carbon Nano tube; [f] nafion

3. RESULT AND DISCUSSION

3.1. Physical characterization

### 3.1.1. Surface characterization of SWNT modified ormosil nanocomposite

Fig 1 (A&B) shows the typical SEM image of ormosil nanocomposite with MB/NAF and SWNT/MB/SnO₂/NAF with adsorbed HRP molecules, respectively. We can see the three dimensional well arranged micro-porous structure of ormosil composite film with MB and nafion, indicating that the matrix is highly porous with an open framework. Therefore, the faster diffusion of substrates and products into and out of the membrane are possible through the interconnected porous channels in the composite film Fig.1 (A). Fig 1(B) shows the adsorption of HRP molecules into the SWNT/MB/SnO₂/NAF modified ormosil composites. The surface became rough after adsorption of enzyme. Spherical SnO_2 particles uniformly dispersed in the matrix with HRP, some cluster type structure also showed that due to coalescence of more than two spherical particles of SnO_2. HRP was strongly adsorbed into the matrix as a brightness structure with SWNT as shown in Fig 1(B). Incorporation of SWNT into the metal oxide derived ormosil matrix increase the electron transfer property and porosity of the nanocomposite film. SEM results also proved that the uniform and open

nanostructure matrix provided a significant increase of effective surface for protein or enzyme loading and a good preparation reproducibility of the biosensor.

Fig. 1 presents the typical AFM image (tapping mode) of MB/SnO$_2$/NAF in ormosil (1.C) and SWNT/MB/SnO$_2$/NAF in ormosil with adsorbed HRP (1.D). Thickness of the MB/SnO$_2$/NAF/Ormosil and SWNT/MB/SnO$_2$/NAF/HRP/Ormosil hybrid films were found to be ~43 and ~300nm, respectively. Film thickness was higher for hybrid film due to incorporation of SWNTs and adsorption of HRP onto the electrode surface. The height difference between the bright region and the dark ground was about 10nm and 50nm for MB/SnO$_2$/NAF/Ormosil and SWNT/MB/SnO$_2$/NAF/HRP/Ormosil hybrid film, respectively. In Fig 1.C, globular shaped tin oxide particles are equally distributed all over the film. However a uniform, stable and regularly patterned compact structure was observed on SWNT/MB/SnO$_2$/NAF/HRP/Ormosil hybrid film, Fig.1.D. The presence of bright spherical shaped structures of HRP in the film indicated that HRP was strongly and uniformly adsorbed on the SWNT modified electrode surface.
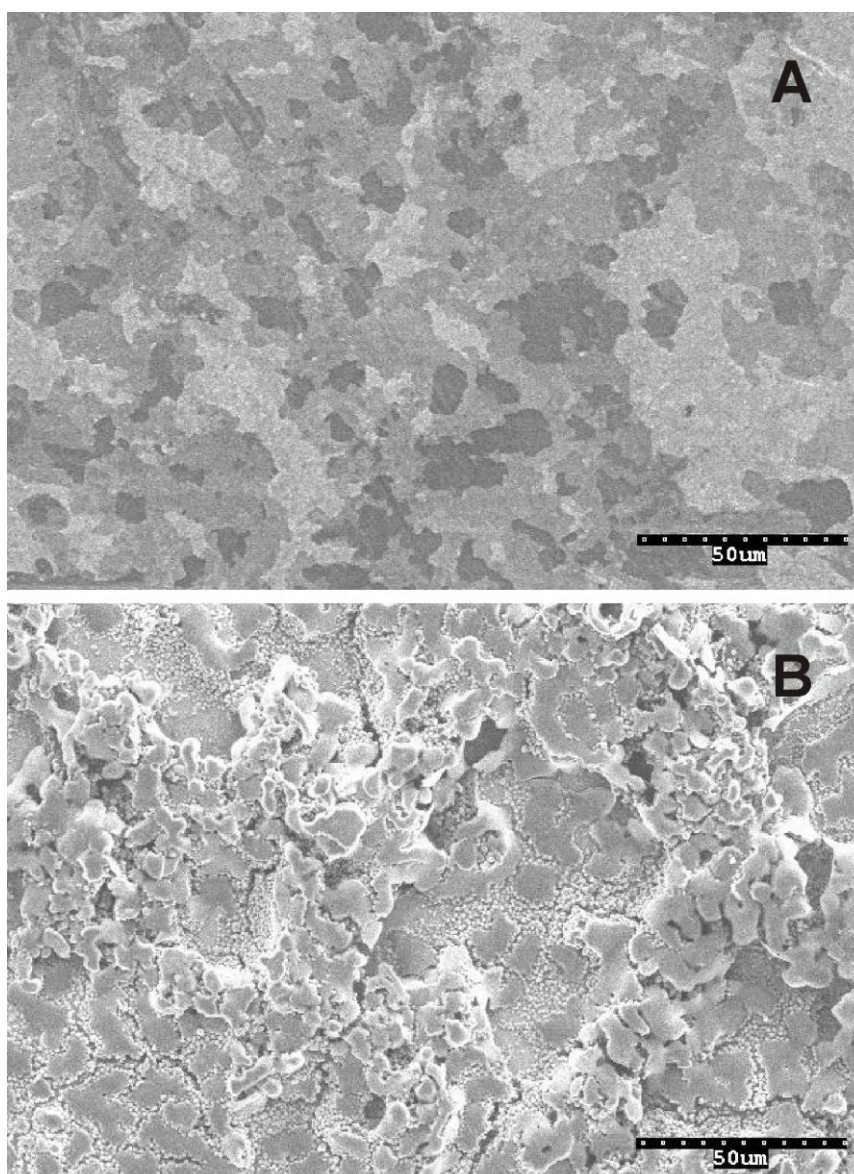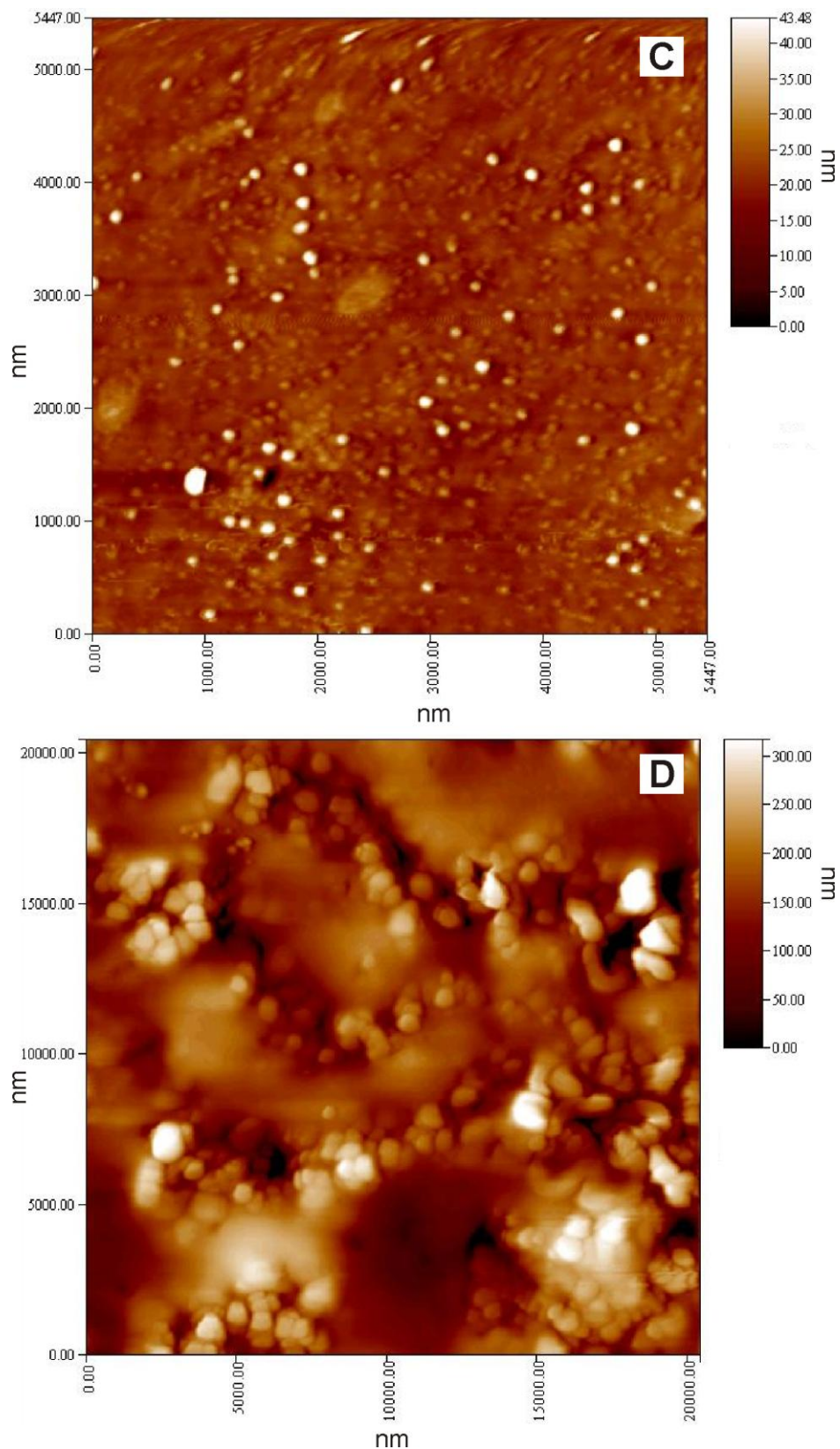
Figure 1. Typical SEM images of MB/NAF/ormosil nanocomposites (A) and SWNT/MB/SnO$_2$/NAF/HRP ormosil nanocomposite film (B) on the surface of ITO glass. AFM images of MB/SnO$_2$/NAF/ormosil (C) and SWNT/MB/HRP/NAF/SnO$_2$ ormosil nanocomposite film (D) on the surface of ITO glass.

*3.1.2. UV-visible of SWNT modified ormosil nanocomposite*

UV-vis spectra can reflect the characteristic structure of proteins. Fig.2 shows UV-vis spectra of the MB in water (curve a), spectra of HRP in water (curve b) and spectra of the adsorbed HRP into the SWNT/MB/SnO$_2$/NAF/ormosil modified film on ITO (curve c) from 300 to 800nm. It was observed that the UV-visible spectrum for the MB was 670 and 615nm (Fig.2, curve a). In the case of MB incorporated with SWNT/SnO$_2$/NAF with adsorbed HRP into ormosil nanocomposites (Fig 2, curve c), the absorption peaks at 670 nm disappeared, due to interaction between MB and silanol groups present in ormosil. Whereas the peak at around 615nm shifted slightly towards lower wavelength at 585 nm (blue shift, by about 30nm). It showed the dimeric form of the dye [31]. The absorption spectra observed at 400nm corresponds to the adsorbed HRP molecules on the electrode surface, which is very closer to the spectra of native HRP. These results revealed that the HRP was successfully adsorbed onto the electrode surface and retained its enzymatic properties in ormosil film in the presence of SWNT/MB/SnO$_2$/NAF.
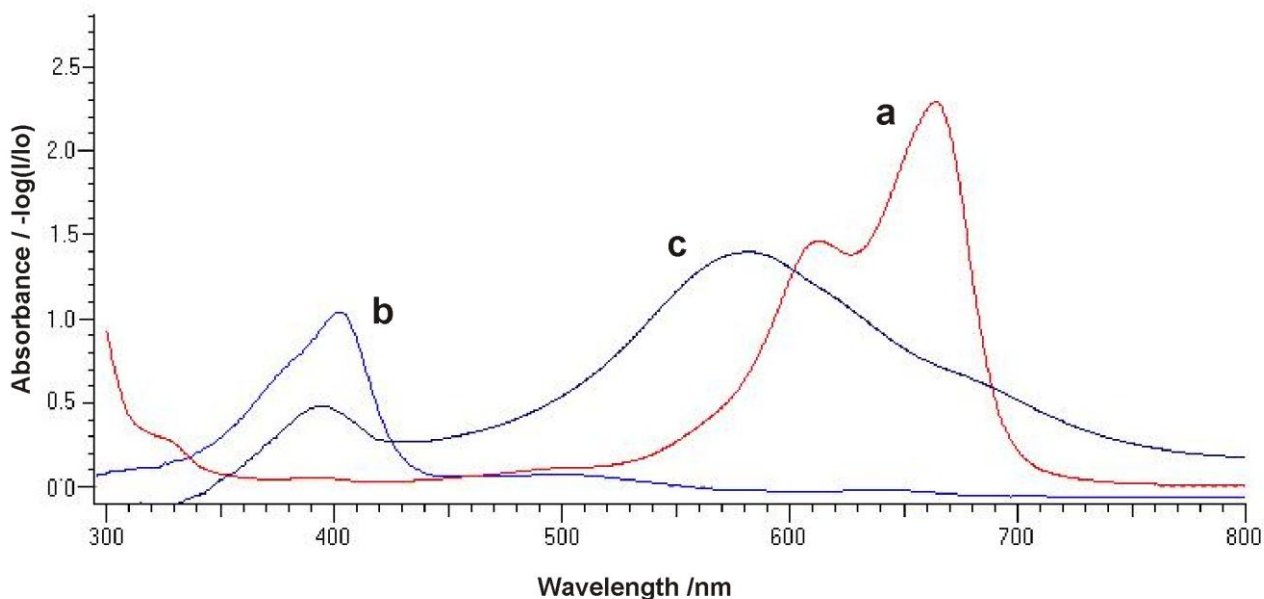
Figure 2. UV-vis spectra of MB solution (a), spectra of HRP in solution (b) and UV-vis spectra of adsorbed HRP into the SWNT/MB/SnO$_2$ ormosil nanocomposite film (c).

3.2. Electrochemical studies of SWNT/MB/SnO$_2$/NAF/HRP,
MB/SnO$_2$/NAF/HRP & SnO$_2$/NAF/HRP on ITO electrode

Fig.3 displays the typical cyclic voltammograms of SWNT/MB/SnO$_2$/NAF/HRP and MB/SnO$_2$/NAF/HRP incorporated into ormosil, over a potential range from 0.0 to -0.4V in 0.1M phosphate buffer solution (pH 7.0) at different scan rates. Fig.3, illustrated the remarkable significance of SWNT in the electrochemical behavior of modified electrodes.
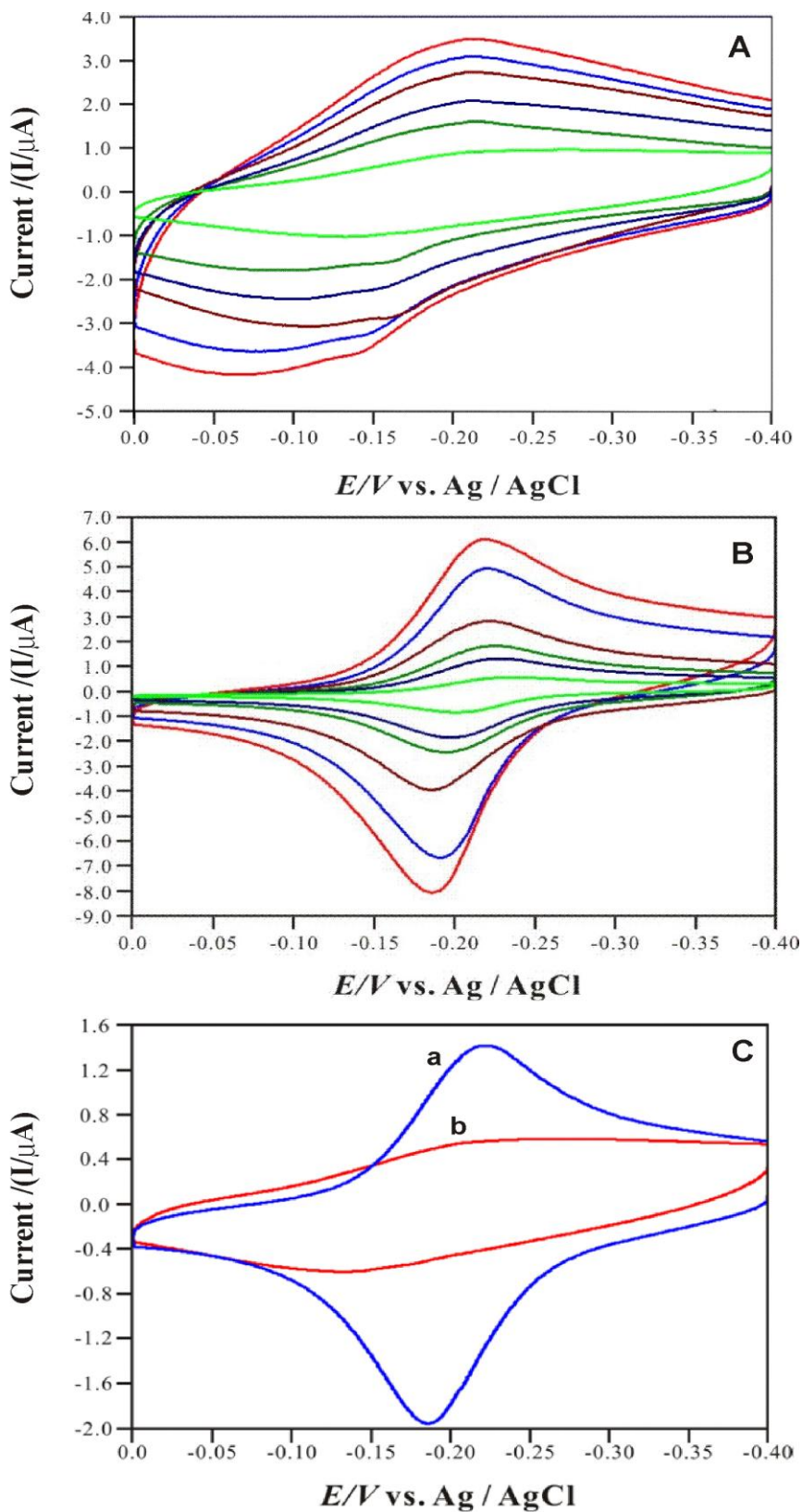
Figure 3. Cyclic voltammograms of MB immobilized into the ormosils in the absence (A) and presence (B) of SWNT in 0.1M PBS (pH 7.0) at the scan rate of 5,10,20,50,100, and 200 mVs^{-1} from inner to outer side. Fig. (C) showed the peak separation of $\Delta Ep=37$ mV for SWNT/MB/SnO$_2$/NAF/HRP (curve a) and $\Delta Ep=70$ mV for MB/SnO$_2$/NAF/HRP (curve b) at the scan rate of 50mVs^{-1} on ITO electrodes.

The modified electrode with SWNT showed a symmetrical well-characterized reversible voltammogram corresponding to the redox reaction of MB. Single walled carbon nanotubes not only increased the peak current, they also improved the redox nature of methylene blue incorporated within ormosil because it increases the effective surface area of modified electrode and provide the maximum space for electrokinetic phenomenon on the surface of modified electrode. The peak separation (ΔE_p) was typically small (~37mV, scanrate-50mV/s, curve a) and the ratio of anodic and cathodic peak current was close to unity for SWNT modified electrode, as shown in fig 3(B) inset. It was clear that the peak potential was independent of the scan rate in the range between 10 and 200mVs^{-1}. The cathodic peak potential and anodic peak potential obtained at SWNT/MB/SnO$_2$/NAF/HRP/ITO were -225mV and -185mV, respectively. The formal potential [$E^{o'}=E_{pa}+E_{pc}$] was -205mV. On the other hand, the MB/SnO$_2$/NAF/HRP showed poor electrochemical response for MB (Fig.3A). As shown, the anodic and cathodic peaks were rather broad and the magnitude of the peak current was significantly lower than that observed on the SWNT/MB/SnO$_2$/NAF/HRP modified electrode. Furthermore, the ΔE_p on the MB/SnO$_2$/NAF/HRP was relatively large (~70mV, scanrate-50mV/s, curve b), suggesting a sluggish electron transfer kinetics. From this result, we confirmed that SWNT/MB/SnO$_2$/NAF/HRP nanocomposites have good electrochemical reversibility. Both the anodic peak current and cathodic peak current were proportional to scan rate at the above scan range, suggesting that peak currents were surface confined. This indicated that redox dye as mediator was immobilized on the surface of the ITO electrode successfully. The electrochemical behavior of SnO$_2$/NAF/HRP was also investigated, but no reversible electrochemical response was observed in the selected potential range due to absence of redox dye MB within the ormosils film (data not shown). MB and SWNT were directly deposited on the ITO electrode without incorporating into ormosils matrix. MB and SWNT molecules at once leached out from the electrode surface and no significant signal was observed (data not shown). To overcome this shortcoming, we used excellent metal oxide derived ormosil matrix to encapsulate the MB, nafion and SWNT to increase the sensitivity and stability of hydrogen peroxide biosensor. Surface coverage (Γ) for the electroactive species was estimated by using Eq. (1)

$$\Gamma = Q/nFA \qquad (1)$$

Where A (0.25cm^2) is the area of the working GCE, n (=1) the number of electron per reactant molecule, Q (2.46x10^{-6}C) the charge obtained by integrating the anodic peak at low voltage scan rate (10 mVs^{-1}), and F is the Faraday Constant. In the present case, the calculated surface coverage for the electroactive species was 1.02x10^{-10} mol cm^{-2}.

3.3. Electrocatalysis of H$_2$O$_2$ on the SWNT/MB/SnO$_2$/NAF/HRP
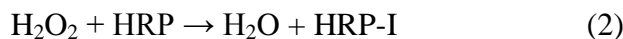*MB/SnO$_2$/NAF/HRP & SnO2/NAF/HRP on ITO electrode*

Fig.4 displays the cyclic Voltammograms of plane MB modified electrode, without addition of H$_2$O$_2$ (curve a), and SnO$_2$/NAF/HRP (curve b), MB/SnO$_2$/NAF/HRP (curve c) and SWNT/MB/SnO$_2$/NAF HRP (curve d) in the presence of 0.3mM H$_2$O$_2$ in 0.1M PBS (pH 7.0) at the scan rate of 50mVs^{-1}. It can be seen (Fig 4, curve c) that a small response was observed for

MB/SnO$_2$/NAF/HRP modified electrode at potential range -0.10 to -0.22 V in the presence of 0.3mM H$_2$O$_2$, but the SWNTs modified electrode SWNT/MB/SnO$_2$/NAF/HRP (curve d) showed a remarkable increase in the cathodic current in the same amount of H$_2$O$_2$ and SnO$_2$/NAF/HRP modified electrode had no significant response (curve b).
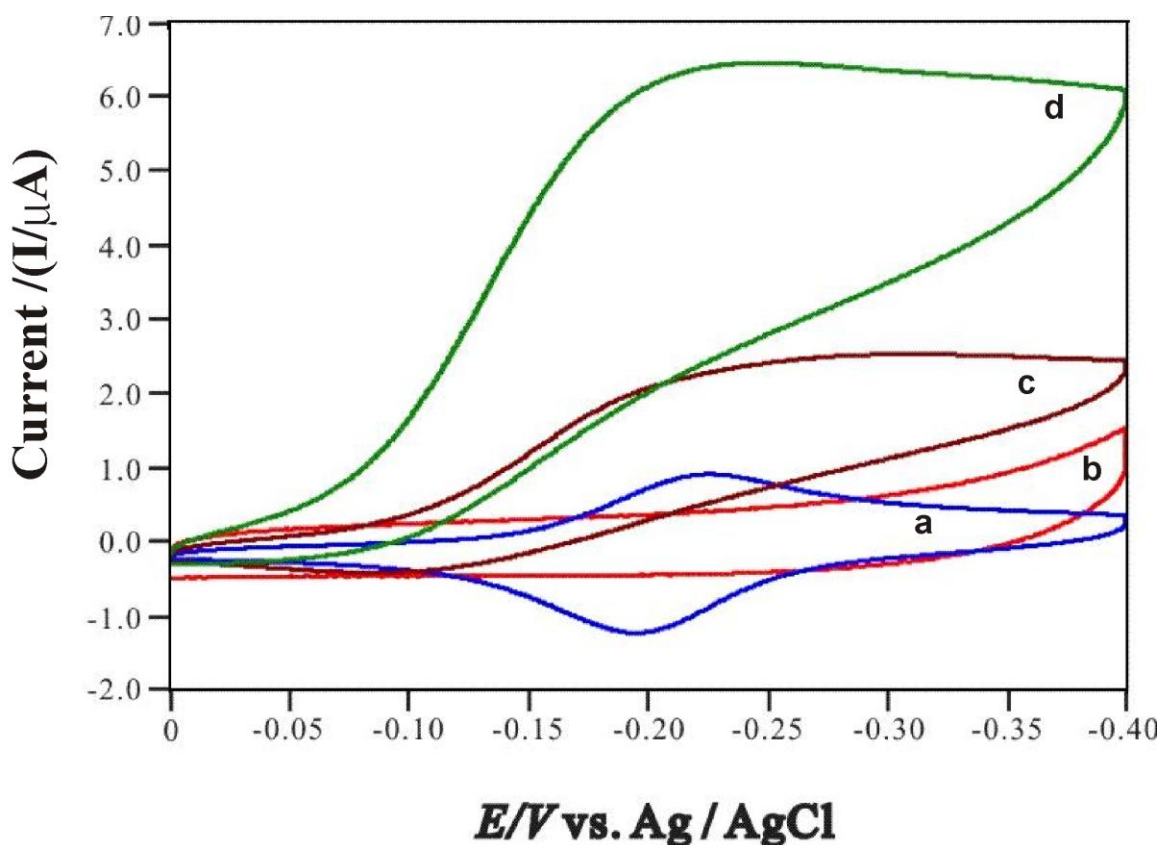

Figure 4. Cyclic voltammograms of (a) plane MB incorporated into ormosil; (b), (c) and (d) are the CVs of SnO$_2$/NAF/HRP, MB/SnO$_2$/NAF/HRP and SWNT/MB/SnO$_2$/NAF/HRP respectively, in the presence of 0.3mM H$_2$O$_2$ in 0.1M PBS (pH 7.0) at the scan rate of 50 mVs^{-1} on ITO electrodes.

The reduction catalytic current of hydrogen peroxide started at -0.05V and obvious catalytic reduction peak appeared at the potential of -0.2 V. SWNT can dramatically enhance the electrochemical response of HRP, resulting in increasing redox currents. This observation illustrated that SWNT played significant role and facilitated the electrocatalysis of hydrogen peroxide on the modified ITO electrode. SWNT not only increased the electrocatalytic current, also lowered the overpotential (~50mV) to reduce the interferences in the measurements. Fig.5 presents the CVs of addition of various concentration of hydrogen peroxide at the scan rate of 50mVs^{-1}in (0.1M, pH 7.0) PBS for SWNT/MB/SnO$_2$/NAF/HRP modified electrode. The cathodic peak current was dramatically increased and anodic peak current disappeared, indicating the fast electrocatalytic reduction of peroxide on the SWNT modified ITO electrode. The mechanism of the sensor can be summarized as follows. The HRP reduces hydrogen peroxide to water.

$$H_2O_2 + HRP \rightarrow H_2O + HRP\text{-}I \qquad (2)$$

Then the oxidized HRP converts MBH to MB^+ and HRP can be regenerated by using a mediator through two separate one-electron steps [32].

$$HRP\text{-}I + MBH \rightarrow HRP\text{-}II + MB^+ + H^+ \qquad (3)$$

$$HRP\text{-}II + MB^+ \rightarrow HRP + MB^+ \qquad (4)$$
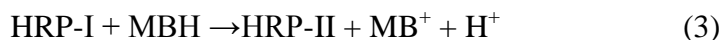
MB^+ reduced at the sensor, results in a cathodic current.

$$MB^+ + H^+ + 2e \rightarrow MBH \qquad (5)$$
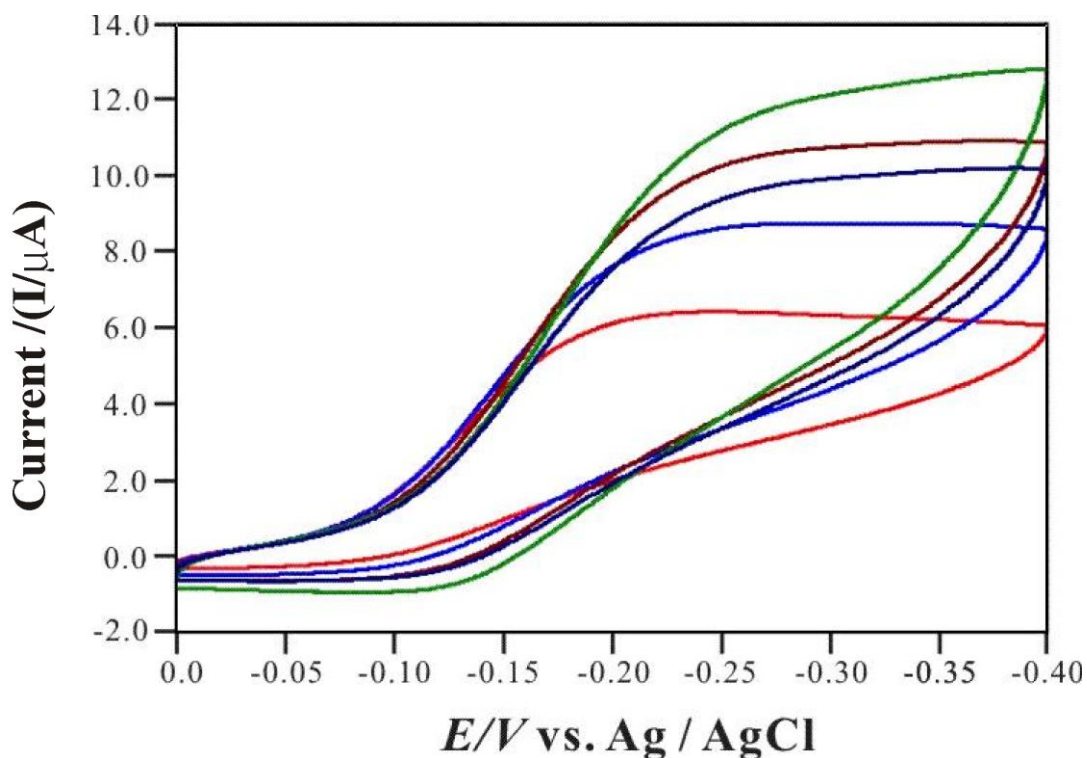
Figure 5. Cyclic voltammograms of SWNT/MB/SnO$_2$/NAF/HRP modified electrode in the presence of different concentration of H$_2$O$_2$; 0.2, 0.4, 0.6, 1.0, 1.2mM in 0.1M PBS (pH 7.0) at the scan rate of 50 mVs^{-1}.

3.4. Optimization of experimental variables

3.4.1. Effect of applied potential and pH on the sensor

The applied potential has an important influence over the sensor response, because the applied potential contributes to the sensitivity and selectivity of the system [33]. Amperometric responses of

the proposed biosensor to H_2O_2 at different potentials were examined in 1.0M, PBS (pH7), as shown in Fig. 6 (A).
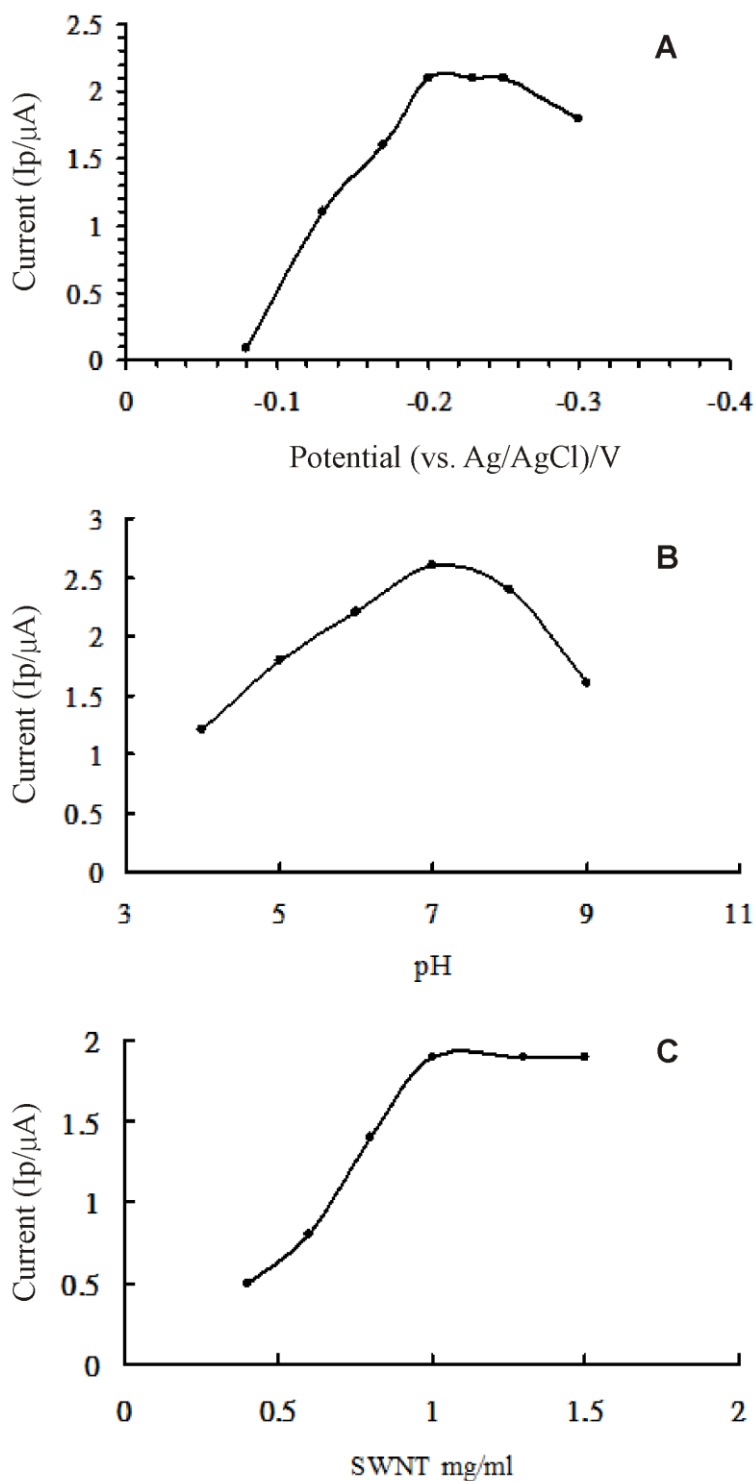
Figure 6. (A) Dependence of catalytic current of the biosensor at different applied potentials measured in pH 7.0 PBS containing 0.3mM H_2O_2. (B) Influence of pH on the H2O2 sensor, study- state current measured in the presence of 0.3mM H_2O_2 in 0.1M PBS (pH 7.0) at applied potential of - 0.2V at 25°C. (C) Effect of SWNTs content on the fabricated biosensor.

The steady-state current increased slowly with applied potential decreasing from -0.08 V to -0.2V which can be attributed to the increasing driving force for the fast reduction of compounds. The current approaches a maximum value at -2.0 V and was constant till -0.25V, and then started to decline. To avoid interferences and reduction of oxygen at high negative applied potential, -0.2.0 V was selected as the applied potential for amperometric measurement. This potential is superior to the previous reported work [34].

The dependence of the biosensor response on pH of the measurement solution was investigated at the applied potential -0.20V, using 0.1 mole l^{-1}, PBS in the presence of (0.3mM) H_2O_2, (Fig.6B). The pH of the solution ranged from 4.0 to 9.0. The current response increased from pH 4.0 and reached the maximum at pH7.0.The current and potential were of the peak depending on the solution pH. Then the current response decreased from pH 7.0 to 9.0. Therefore, the suitable pH with the maximum activity of the adsorbed HRP on the electrode surface was at pH 7.0, which was in agreement with that reported for soluble HRP [35].

3.4.2. Effect of temperature and SWNT content on the sensor

The effect of temperature on the sensor was examined between 15 to 50°C. The response signal of the H_2O_2 sensor increased as the temperature varied from 15 to 35°C. But at temperature lower than 20°C, the activity of the enzyme was rather lower and the response time was relatively longer. On the other hand, at temperatures higher than 35°C, the activity of enzyme decreased rapidly due to the partial denaturation of the enzyme. Taking both the lifetime and response time into consideration, 25°C was the selected temperature for the fabrication of biosensor.

The influence of SWNTs content was also investigated for the fabrication of H_2O_2 biosensor because it played significant role in the electroreduction of hydrogen peroxide on the modified electrode surface. As shown in Fig 6(C), the current response started to increase from 0.4 to 1.0 mgml^{-1} of SWNT content. Afterwards, it became constant till 1.5 mgml^{-1} of SWNT content. So the 1.0 mgml^{-1} SWNTs content was selected for the fabrication of H_2O_2.

3.4.2. Kinetic analysis:

The apparent Michaelis-Menten constant (K_M), which gives an indication of the enzyme-substrate kinetics, can be calculated from the electrochemical version of the Lineweaver-Burk equation

$$1/ I_{ss} = 1/ I_{max} + K_M / I_{max} \text{ x } 1/C \qquad (6)$$

Where I_{ss} is the steady-state current after the addition of substrate, *C* is the bulk concentration of the substrate and I_{max} is the maximum current measured under saturated substrate condition. The K_M value was determined by analysis of the slope and intercept for the plot of the reciprocals of the cathodic current versus H_2O_2 concentration. The K_M value of the H_2O_2 sensor was determined by steady-state amperometric response and found to be 1.6mM. This value was lower than those of

4.6mM for HRP immobilized in sol-gel/hydro gel modified electrode [36], 4.51mM for HRP on AuNP/CHIT/SPCE [37], 4.04mM for HRP on TTF/TCNQ/MWCNT modified electrode [38], 5.12mM for SBP (soybean peroxidase) immobilized in sol-gel thin film [39] and was close to 2.0mM for HRP immobilized on FMC-BSA/MWCNT ormosil composite-modified GC electrode [40].The smaller value of K_M means that the immobilized HRP possesses higher enzyme activity, and the present modified electrodes exhibit higher affinity to H_2O_2.

4. ANALYTICAL CHARACTERIZATION OF FABRICATED H_2O_2 BIOSENSOR
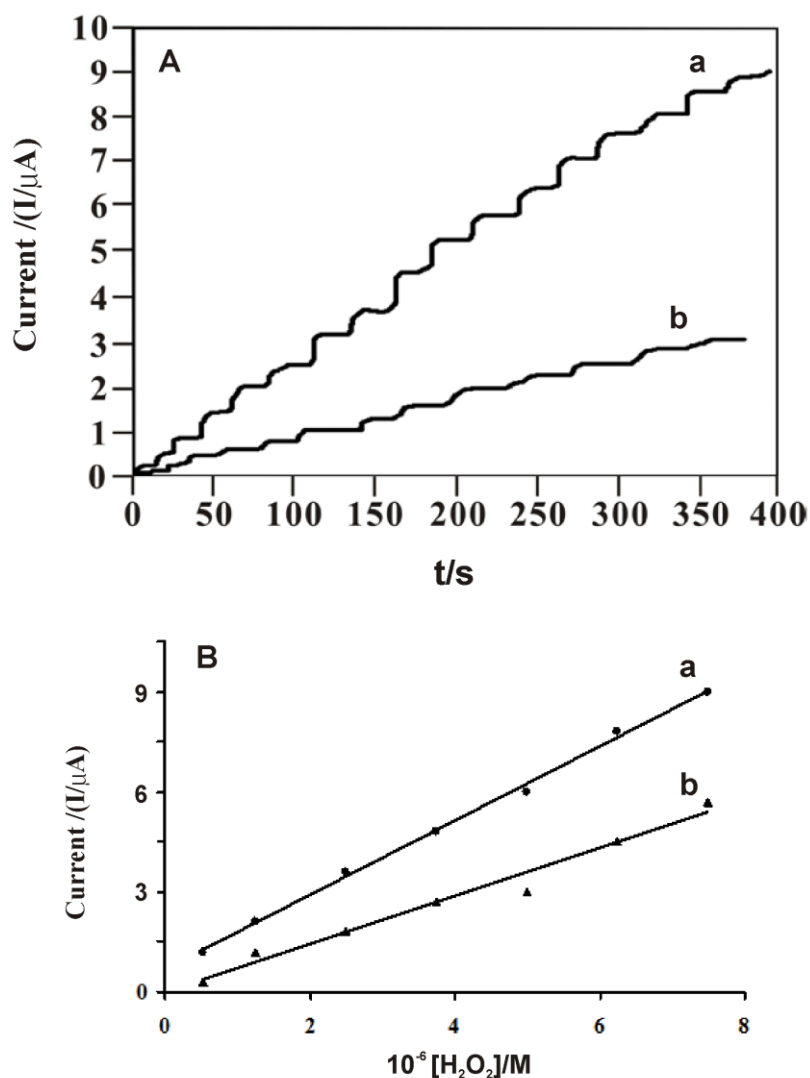
Figure 7. (A) Amperometric response of (curve a) SWNT/MB/SnO$_2$/NAF/HRP and (curve b) MB/SnO$_2$/NAF/HRP in a stirred 0.1M PBS (pH 7.0) after successive hydrogen peroxide additions at applied potential -0.2V vs. Ag/AgCl. In Fig.8 (B) shows the linear calibration plot of catalytic currents vs. hydrogen peroxide concentrations (curve a) SWNT/MB/SnO$_2$/NAF/HRP, where y=0.9706x+0.2256, R^2=0.9977 and (curve b) MB/SnO$_2$/NAF/HRP, where y=0.6389x+0.0006, R^2=0.9742.

Figure 7 presents the dynamic amperometric response of the sensor at a working potential of -0.2V with successive injections of 0.3mM H_2O_2 in 0.1M PBS (pH7.0) on MB/SnO$_2$/NAF/HRP, SWNT/MB/SnO$_2$/NAF/HRP and SnO$_2$/NAF/HRP. The trace clearly demonstrated the fast response and high sensitivity of the SWNT/MB/SnO$_2$ /NAF/HRP to H_2O_2 than MB/SnO$_2$/NAF/HRP and SnO$_2$/NAF/HRP, suggesting that the SWNTs facilitated the electron transfer in the matrix and enhanced the electrocatalytic properties of modified electrode. The response time was less than 5s (t=95% of I_{max}), which was much lower than the earlier reported for H_2O_2 biosensor [41]. Fig 7, (inset) displayed the calibration plot of the SWNT based biosensor. The response to H_2O_2 was linear in the range from 5×10^{-7} to 1×10^{-4}M with a correlation coefficient of 0.998 (n = 10), with the lower detection limit of 0.3μ M (S/N=3). The higher sensitivity of the sensor may result from the biocompatible microenvironment around the enzyme [42]. The linear range, response time and limit of detection observed with SWNT/MB/SnO$_2$/NAF/HRP modified electrode is in general comparable with most of the modified electrode reported in the literature(Table 2) [43-45].The recovery rate was also estimated with the basic method of slandered recovery test. The recovery data were obtained as 98.6%.

4.1. Stability of the developed H_2O_2 biosensor

The stability of the biosensor was examined by amperometric measurements in the presence of 10μM H_2O_2 periodically. It was found that the response of the biosensor maintained about 90% of the initial values after 90 days. When biosensor was not in use, it was stored under dry condition at 4°C in a refrigerator. The good long term stability can be attributed to the great stability of MB and the excellent biocompatibility and the stabilizing microenvironment around the HRP provided by the SWNT and metal oxide based organically modified sol-gel composite matrix.

Table 2. Comparison of the efficiency of SWNT/MB/SnO$_2$/NAF/HRP modified electrode used in determination of H_2O_2.

Electrode	Method	Electrolyte	LOD[a]	LCR[b] (M)	RT[c] (Sec)	Ref.
SWCNT/CTAB/HRP/GCE	CV	pH 7 PBS	3.6μM	1.2×10^{-5}-1.4×10^{-4}	4	43
SWCNT /Au-Nps/PPy/HRP	CV	pH 7 PBS	0.5μM	5×10^{-5}-1×10^{-3}	<8	44
SWCNT/PB/HRP/GCE	CV	pH 6.8PBS	0.64μM	up to 2×10^{-3}	10	20
SWCNT/CHIT/HRP /GC	CV	pH 6.8PBS	3μM	25×10^{-6}-3×10^{-4}	6	17
SG/MG/Nafion/HRP/GCE	CV	pH 7 PBS	0.1μM	5×10^{-7}-1.6×10^{-3}	20	24
MWCNT/CHIT/SG/HRP	CV	pH 7.4 PBS	1.4μM	4.8×10^{-6}-5×10^{-3}	5	45
MWCNT/TB/HRP/GCE	CV	pH 7 PBS	1.7μM	up to 4×10^{-3}	8	14
SWNT/MB/SnO$_2$/NAF/HRP	CV	pH 7 PBS	0.3μM	5×10^{-7}- 1×10^{-4}	<5	Present work

[a]LCR- Linear concentration range, [b]LOD- Limit of detection, [c]RT- Response time.

4.2. Selectivity against interferences

The interferential experiment of the fabricated H_2O_2 biosensor was performed by comparing the amperometric response of 0.3mM H_2O_2 before and after adding some possible interferents into

0.1M pH 7.0 PBS solutions. Glucose, cystine and uric acid did not interfere with the determination of H_2O_2 (table 3). However, an obvious interference was observed, when 10-fold ascorbic acid and citric acid were added. The reason may be that the ascorbic acid/citric acid can be oxidized by MB. So, the oxidation form of the MB can be reduced and the circulation catalytic reaction is destroyed [43]. Dopamine and NADH had no significant effect on the prepared SWNT/MB/SnO$_2$/NAF/HRP based peroxide biosensor.

Table 3. Interferences studies

Interferents	Current ratio
Uric acid	1.00
Glucose	1.00
Cysteine	1.00
Dopamine	0.98
Ascorbic acid	0.90
NADH	1.00
Citric acid	0.94

5. CONCLUSIONS

We have developed a novel SWNT /Ormosil based electrochemical biosensor for the analytical detection of hydrogen peroxide. SWNT, nafion and MB were successfully incorporated within ormosils matrices and HRP was adsorbed onto the electrode surface diffusionally. The experimental results proved that SWNT facilitated the electrocatalytic reduction of H_2O_2 on the electrode surface. The modified electrode SWNT/MB/SnO$_2$/NAF/HRP shows stable and reproducible electrochemical behavior, long stability and excellent electrochemical reversibility. SWNT based biosensor showed excellent electrocatalytic activity for H_2O_2 reduction at reduced over potential with fast response time (<5sec) with very low limit of detection (0.3μM). So, this novel and efficient strategy, opens up a new approach to construct of variety of SWNT based organically modified sol-gel glasses amperometric biosensors.

References

1. X.H. Shu, Y. Chen, H.Y. Yuan, S.F.Gao, D. Xiao, H_2O_2 , *Anal. Chem*., 79 (2007) 3695-3702.
2. L. Wang, E. Wang, A , *Electrochem. Commun*., 6 (2004) 225-229.
3. N.V. Klassen, D. Marchington, H.C.E. McGovan**,** H_2O_2 **,** *Anal. Chem*., 66 (1994) 2921-2925.
4. A.Lobnik, M. Cajlakovuc, , *Sens. Actu. B Chem*., 74 (2001) 194-199.
5. S.H. Chen, R. Yuan, L.Y. Zhang, N. Wang, X.L. Li, , *Biosens. Bioelectron*., 22 (2007) 1268-1274.

6. T. Gu, Y. Liu, J. Zhang, Y. Hasbebe, , *J. Enviro. Sci.*, 21(2009) S56-S59.
7. W. Li, R. Yuan, Y. Chai, L. Zhou, S. Chen, Na Li., , *J. Biochem Biophys. Methods*, 70(2008) 830-837.
8. C.X. Lie, S.Q. Hu, G.L. Shen, R.Q. Yu, , *Talanta*, 59 (2003) 981-988.
9. Y. Song, L. Wang, C. Ren, G. Zhua, Z. Li, , *Sens. Actuat. B Chem.*, 114 (2006) 1001-1006.
10. S. Kevyn, J.S. Nathan, R.R. Kenton, E.E. Timothy, M. Castro, M.R. Parkar, , *J. Am. Chem. Soc.*, 124 (2002) 4247-4252.
11. X. Chen, B. Wang, S. Dong, ,*Electroanalysis,* 13 (2001) 1149-1152.
12. S. Iijima, , *Nature,* 354 (1991) 56-58.
13. Y. M. Yan, O. Yehezkeli, I. Willner, , *Chem. Eur. J.*, 13 (2007) 10168-10175.
14. Y. Liu, J. Lei, H. Ju, , Talanta, 74 (2008) 965-970.
15. X. Yu, B. Munge, V. Patel, G. Jensen, A. Bhirde, J. D. Gong, S. N. Kim, J. Gillespie, J.S. Gutkind, J.S. Rusling, , *J. Am. Chem. Soc.*, 128 (2006) 11199-11205.
16. A.Salimi, L. Miranzadeh, R. Hallaj, H. Mamkhezri, , *Electroanalysis*, 20(2008) 1760-1768.
17. H. J. Jinag, H. Ynag, D. L. Akins, , *J. Elec. Ana. Chem.*, 623 (2008) 181-186.
18. A.Choi, H. Jeong, S. Kim, S. Jo, S. Jeon, , *Electrochim. Acta*, 53 (2008) 2579-2584.
19. M. C. Kum, K. A. Joshi, W. Chen, N. V. Myung, , *Talanta*, 74(2007) 370-375.
20. A.Arvinte, L. Rotariu, C. Bala, A. M. Guraban., , *Bioelectrochemistry*, 76(2009) 107-114.
21. X. Yang, Y. Lu, Y. Ma, Z. Liu, F. Du, Y. Chen, , *Biotech. Lett.*, 29 (2007) 1775-1779.
22. K. M. Shin, J. W. Lee, G. G. Wallace, S. J. Kim, , *Sens. Actua. B Chem.*, 133 (2008) 393-397.
23. J. Tkac, T. Ruzgas, , Electrochem. Commu., 8 (2006) 899-903.
24. A.K. Upadhyay, Tzu-Wei Ting, S.M. Chen, , *Talanta*, 79 2009 38-45.
25. J. Manso, M.L. Mena, P. Yanez-Sedeno, J. Pingarron, , *J. Electroanal. Chem.*, 603 (2007) 1-7.
26. A.Salimi, L. Miranzadeh, R. Hallaj, H. Mamkhezri, , *Electroanalysis*, 20 (2008) 1760-1768.
27. H. N. Choi, M. A. Kim, W. Y. Lee, *Anal. Chim. Acta*, 537 (2005) 179-187.
28. D.Avnir, O. Lev, J. Livage, , *Journal of Mater. Chem.*, 16 (2006) 1013-1030.
29. T. Coradin, J. Livage, , *Accounts of Chemi. Res.*, 40 (2007) 819-826.
30. X. Chen, S. Dong, , *Biosens. Bioelectron.*, 18 (2003) 999-1004.
31. S. Jockusch, N. J. Turro, , *Macromolecules*, 28 (1995) 7416-7418.
32. K. Aoki, H. Kaneko, , *J. Eelectroanal. Chem.*, 247 (1988) 17-27.
33. E. Csoregi, G. Jonsson-Petersson, L.Gorton, , *J. Biotechnol.*, 30 (1993) 315-337.
34. A.K.M Kafi, G. Wu, A.Chen, , *Biosens. & Bioelectro.*, 24 (2008) 566-571.
35. G.H. Wang, L.M.Zhang, , *J. Phys. Chem.* B, 110 (2006) 24864-24868.
36. B. Wang, J. Zhang, G. Cheng, S. Dong, , *Anal. Chim. Acta.*, 407 (2000) 111-118.
37. T. Tangkuaram, C. Ponchio, T. Kangkasomboon, P. Katikawong, W. Veerasai, , *Biosen. Bioelectro.*, 22 (2007) 2071-2078.
38. Z. Cao, X. Jiang, Q. Xie, S. Yao, , *Biosen. Bioelectro.*, 24 (2008) 222-227.
39. Q. Wang, G. Lu, B. Yang, , *Anal. Chem.*, 71 (1999) 1935-1939.
40. L. Ma, R. Yuan, Y. Chai, S. Chen, ,*J. Mole. Cata. B*, 256 (2009) 215-220.
41. H.Yao, N. Li, S. Xu, J. Zhong, J-J. Zhu, H-Y. Chen., , *Biosens. & Bioelectro.*, 21 (2005) 372-377.
42. B. Q. Wang, B. Li, Q. Deng, S. J. Dong, *Anal. Chem.*, 70 (1998) 170-174.
43. G.Wang, J.J. Xu, H.Y. Chen, Z.H. Lu., , *Biosens. & Bioelectro.*, 18 (2003) 335-343.
44. S. Wang, F. Xie, G. Liu, s, *Talanta,*77 (2009) 1343-1350.
45. L. Zhu, R. Yang, J.Zhai, C. Tian, , *Biosens. Bioelectro.*, 23 (2007) 528-535.